

Dual wavelength endoscopic laser speckle contrast imaging system for indicating tissue blood flow and oxygenation

Lipei Song*, Daniel S. Elson

Hamlyn Center for Robotic Surgery and Department of Surgery and Cancer, Imperial College London, UK

ABSTRACT:

We present a dual-wavelength endoscopic laser speckle contrast system including illumination with polarization maintaining fibres and imaging using a leached fibre image guide. This system has a frame rate of 10 Hz and can rapidly monitor changes in blood flow in vivo, including due to the heart beat, using the contrast values of the speckle images recorded with 1 ms exposure time. In addition the mean intensities can record the respiration period and can indicate changes in tissue oxygenation. This system was tested during an occlusion to a human finger and is being applied in endoscopy.

Key words: Laser speckle contrast, oxygenation, dual wavelength speckle, heart beat rate, respiration

1. INTRODUCTION

The survival of cells depends on sufficient nutrition and oxygenation from the arterioles and the disposal of metabolic waste through the venules. A lack of blood supply threatens the health of the cells and leads to various diseases or impedes tissue recovery and may be a result of circulatory pathology. Therefore investigating the circulation is helpful for diagnosing disease^[1-5], assessing recovery^[6] and helping to understand haemodynamics and oxygenation levels. Photoplethysmography (PPG)^[7], pulse oximetry, and electrocardiography (ECG) can all detect the cardiac cycle. Alternatively, laser Doppler flowmetry^[8, 9], laser speckle contrast analysis (LASCA)^[10, 11], and angiography may be used to indicate the blood flow by detecting the motion of scattering particles, i.e. red blood cells. Multiwavelength imaging using tunable light sources or filter wheels or tunable filters allows imaging of the reflectance spectra of tissues^[12] from which oxygenation saturation can be measure and monitor. However it will be helpful to have a system which can monitor all these factors. In addition, the application of optical methods is limited by the visible light penetration depth which is around a few millimetres or less and monitoring the blood flow within the body demands an endoscopic system. In our previous work we investigated an endoscopic laser speckle analysis system based on a leached fibre image guide (LFIG) and showed that it is possible to image the circulation structure using a data processing method, Butterworth low pass filter or defocusing the LFIG in a small range for different speckle size, to remove the structure of fibre bundle and retrieve the speed distribution^[13].

In this paper we present an endoscopic laser speckle contrast imaging system (eLASCA) using two illumination wavelengths to monitor the blood flow and indicate changes in oxygenation. The system has been demonstrated using the occlusion of a human finger to monitor the blood flow and show signal changes at the heart beat frequency and the respiration period, as well as the oxygenation status based on the changes of concentration of oxygenated haemoglobin (HbO₂) and deoxygenated haemoglobin (HbR).

2. METHODS

2.1 Experiment design

The probe, shown in Fig. 1 (a) was designed including two polarization maintaining fibres (PM fibre, Thorlabs) that connect to two laser diodes (ML101J27 660 nm and DL8142 830 nm, Thorlabs) to illuminate a sample area. A plano-convex lens ($f=6\text{mm}$, $D=3\text{ mm}$, Edmund Scientific) was placed between a polarizer and the near end of a leached fibre image guide (LFIG). The polarization direction of the two PM fibres was adjusted to be

perpendicular to that of the polarizer to eliminate the specular reflection from the sample. The position of the LFIG (Schott North America) can be adjusted within the probe to acquire different magnifications. The diameter of the probe is 10 mm and the length is 50 mm. The field of view (FOV) in our experiment was adjusted to be around 15 mm in diameter to image the whole of a human fingertip. Fig 1 (b) shows the experimental set up. The light scattered from the fingertip was imaged onto the LFIG in the probe. The image transmitted through the LFIG and was imaged onto a CCD after a x5 magnification system consisting of a microscope objective (x20, Olympus) and an achromatic lens (f=100mm, Thorlabs). The position of the far end of the LFIG was adjusted to be slightly out of focus to remove the fibre bundle structure but maintain the lower resolution image information from the sample. According to our previous work this also improves the sensitivity of the system and saves data processing time [13]. A motorized fast filter wheel (Thorlabs, FW103H) alternately introduced two bandpass filters (FB650-40 and FB830-10, Thorlabs) into the optical path to acquire images with the two laser diodes respectively and reject background light. The system was controlled by a custom LabVIEW program. Because the settling time of the filter wheel, the frame rate of dual wavelength images was limited to 4 frames per second (fps). This is too low to capture the heartbeat, therefore both wavelengths were used to indicate average oxygen saturation, but only one wavelength, 660 nm was used for detecting heart beat. The images were 2x2 binned to improve the frame rate.

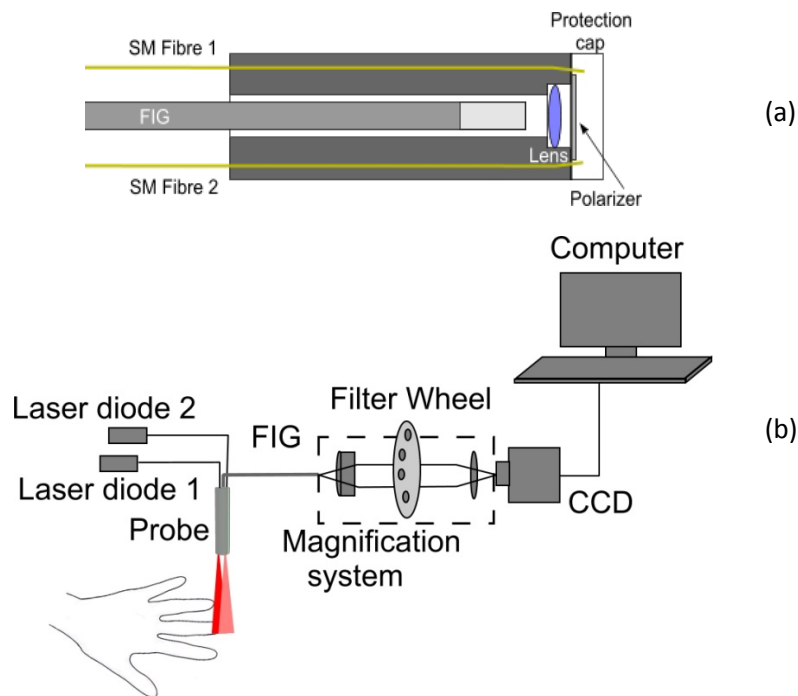


Figure 1. (a) The probe design; (b) Experiment setup

2.2 Blood flow speed, cardiac cycle and respiration

A blood pressure cuff was placed around the arm and inflated to change the blood circulation and oxygenation saturation in the fingers. When the vessels were occluded, the blood flow speed is expected to decrease and hence results in higher speckle contrast values. The contraction and relaxation in the cardiac cycles changes the blood pressure and the blood flow speed in the vessels. In addition the vessel walls also move synchronously with the fluctuation of blood pressure because of its elasticity^[14]. Both of these phenomena are expected to affect the laser speckle results.

Respiration modulates the blood volume by changing the intrapleural pressure, which increases and decreases the venous return and the cardiac output consequently^[15, 16]. Therefore the reflected light from the tissue changes synchronously with the ventilation rate^[7].

In the first experiment 500 images were acquired using the 660 nm laser starting 15 seconds after the cuff was fully inflated, lasting for around 40 seconds. The exposure time of the CCD was 1 ms and the frame rate was 17 fps. Then the cuff was deflated and the fingers were rested for 20 seconds for the blood circulation recovered. Then another set of 500 frames was recorded. During both of the data acquisition periods the subject was asked to maintain the respiratory cycle to be about 8 seconds.

During data processing the contrast map of the speckle images was calculated using the standard deviation and mean value within a moving 7×7 kernel window. The average contrast of each frame as well as the mean intensity in the area of interest (AOI) were also calculated to investigate the change of blood flow speed change, heart beat rate and respiration. A fast Fourier transform (FFT) was applied to both the DC detrended intensity change and the contrast change for the modulation frequency.

2.3 oxygenation calculation

Assuming that HbO₂ and HbR are the main contributors to the absorption of the light in tissue, the occlusion of the vessels changes the concentration of these two chromophores and the collected intensity at these two wavelengths. According to the absorption coefficient curves^[17] in Fig. 2, 660nm and 830 nm are at either side of an isobestic point of the haemoglobin absorbance.

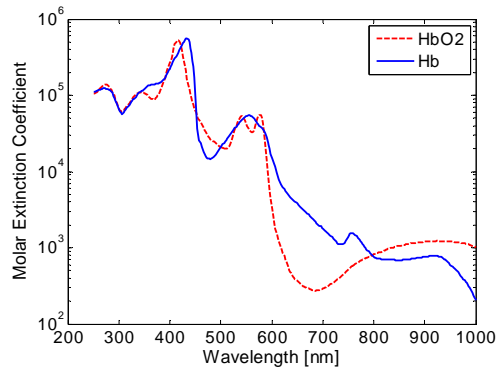


Figure 2. Molar extinction coefficient of the hemoglobin in water [Reference]

The oxygenation can be approximately evaluated by the concentration changes of the oxygenated haemoglobin (HbO₂) and deoxygenated haemoglobin (HbR) according to the Beer-lambert law^[18, 19], assuming that the wavelengths probe a similar volume of tissue:

$$\begin{bmatrix} \Delta H_{bO_2}(t) \\ \Delta H_{bR}(t) \end{bmatrix} = \begin{bmatrix} \epsilon_{H_{bO_2}}^{\lambda_1} & \epsilon_{H_{bR}}^{\lambda_1} \\ \epsilon_{H_{bO_2}}^{\lambda_2} & \epsilon_{H_{bR}}^{\lambda_2} \end{bmatrix} \begin{bmatrix} \frac{\ln(R_{\lambda_1}(0))/\ln(R_{\lambda_1}(t))}{L_{\lambda_1}(0)} \\ \frac{\ln(R_{\lambda_2}(0))/\ln(R_{\lambda_2}(t))}{L_{\lambda_2}(0)} \end{bmatrix} \quad (1)$$

Where ϵ refers to the molar extinction coefficient of the chromophores which are HbO₂ and HbR in our experiment at the two wavelengths. R is the experimental intensity data and L is the differential path length factor. Here, due to the unknown parameter L, we only consider the relative change of HbO₂ and HbR.

The change of the blood volume is approximated by evaluating the change of the total haemoglobin concentration which is calculated as^[18]:

$$\Delta Hb(t) = \Delta H_{bO_2}(t) + \Delta H_{bR}(t) \quad (2)$$

The relative haemoglobin saturation SO₂ is calculated as^[20]

$$SO_2 = \frac{H_b O_2(t)}{H_b O_2(t) + H_b R(t)} \quad (3)$$

During the second experiment, the exposure time of the CCD was set 5 ms to improve the signal to noise rate (SNR). The experimental procedure was the same as that for the blood flow measurement but only 100 frames for each wavelength were recorded. Then the oxygenation saturation was calculated based on the mean intensity of the AOI at each wavelength.

3. RESULTS

Fig. 3 (a) shows the raw speckle image recorded by the CCD and the contrast map after data processing. The bright area is the LFIG and the border of the finger can be seen. Fig. 3 (b) shows the contrast image. The contrast decreases from the middle of the fingertip to the border. The low contrast area shown in red at the corner of the contrast image came from the CCD noise. The black square in Fig. 3(b) shows the AOI where the mean contrast and mean intensity were calculated.

Fig. 4(a) shows the contrast change in the fingertip due to the occlusion and release of the forearm. A number of observations may be made from this data. Firstly, when the forearm was occluded, the blood flow speed was lower, which generated higher speckle contrast. After the cuff was deflated, the circulation returned to normal and the speckle contrast decreased, which we believe is due to a higher blood flow speed during the draining of the blood throughout the tissue and veins. Secondly, the contrast oscillated over a larger range when the cuff was inflated compared with when it was deflated. From the temporally expanded picture shown in Fig. 4(b) we can see that the contrast fluctuates with two characteristic periods. The faster frequency corresponds to the cardiac cycle and the slower one is similar to the respiratory period. This is clearly observable in the FFT data in Fig. 4(d) where the faster frequency is 1.2 corresponding to 72 beats per minute, and the slow frequency is 0.125, as expected. Fig. 4(c) shows the mean intensity of the AOI when the flow was occluded. The mean intensity oscillates with a period of less than 10 seconds. The FFT of the mean intensity of Fig. 4(c) is shown in Fig. 4 (d) as the red line. The spectrum of the mean intensity overlaps with that of the contrast at the frequency of the 0.125.

The results of haemodynamic information are shown in Fig. 5(a) and (b). In Fig. 5(a) the concentration of the HbO₂ increased after the blood flow was released and at the same time the concentration of HbR decreased. The reason for this is that the deoxygenated blood accumulates in the finger due to venous occlusion. When the occlusion is released, the deoxygenated blood flows out of the finger and induces less concentration of the HbR. This also explains the trend in oxygen saturation, which is shown in Fig. 5(b).

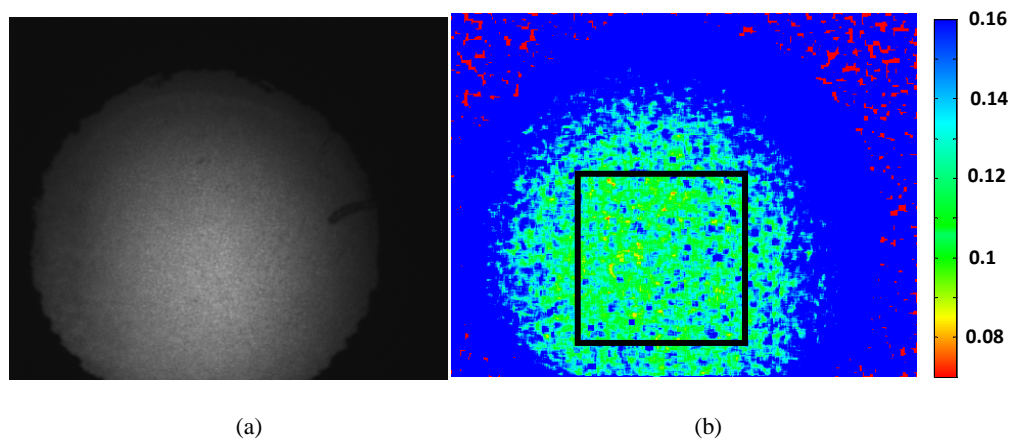


Figure 3 (a) Speckle image; (b) contrast map of XXX. The black rectangle in (b) shows the AOI for averaging the contrast values and pixel intensities. A video sequence of contrast map showing the blood pulsation was acquired.

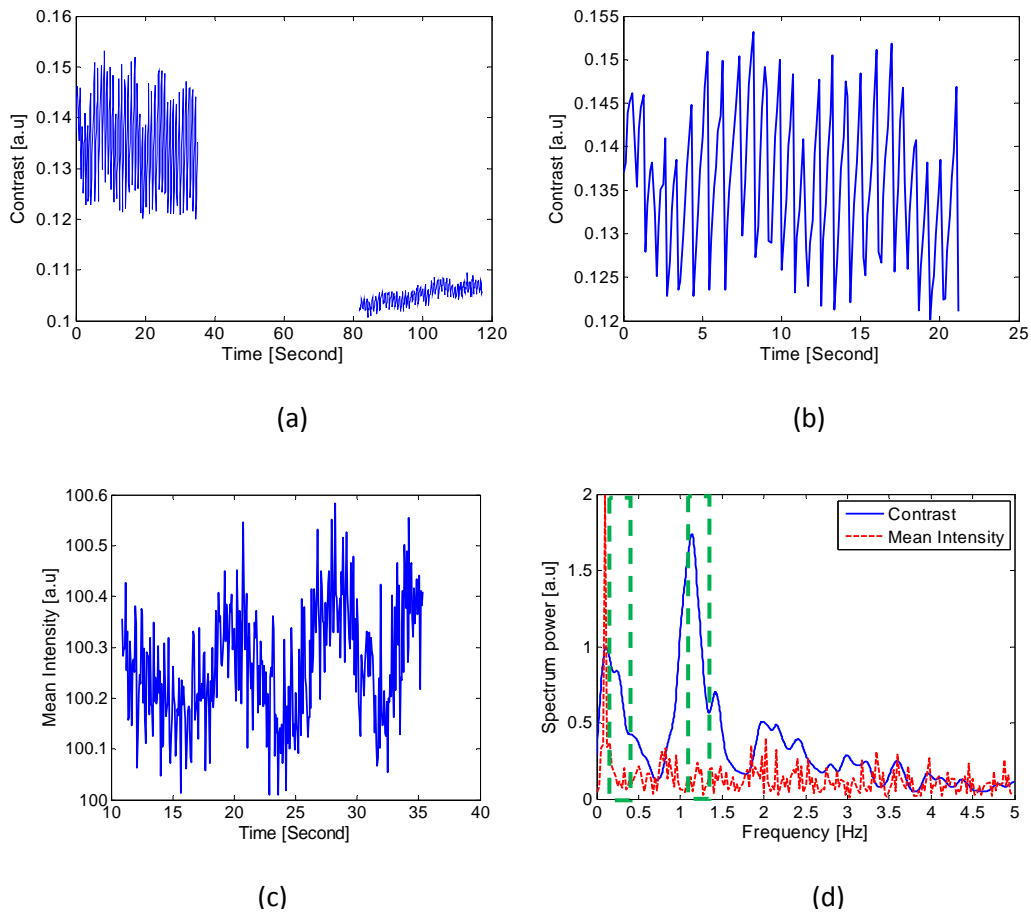


Figure 4. (a) Averaged contrast; (b) zoomed in contrast for the first 22 seconds; (c) mean intensity; (d) spectral power of the contrast and mean intensity

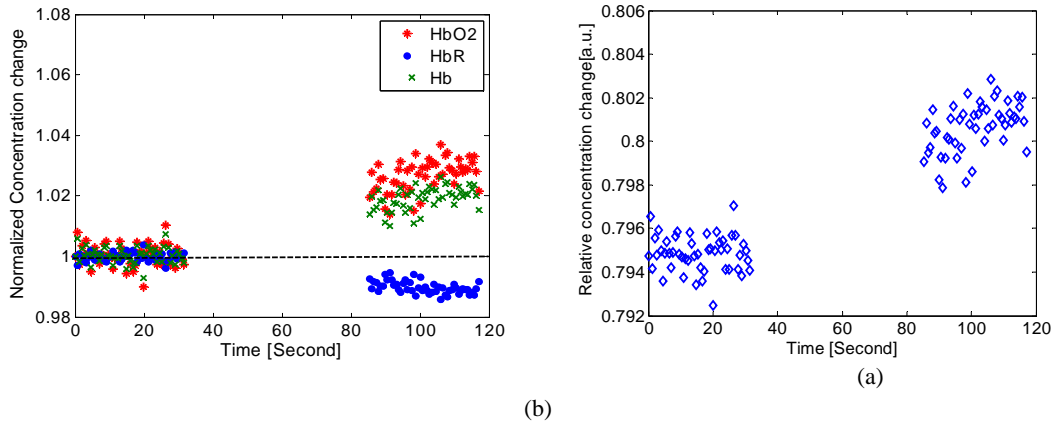


Figure 5. (a) Normalized concentration change before and after the occlusion; (b) relative oxygen saturation change in the experiment.

4. DISCUSSION AND CONCLUSION

As mentioned, the interaction between the light and the tissue is complex. In a cardiac period not only the blood volume, the blood flow speed and the oxygenation saturation change, but also the vessel walls move. All of

these factors can affect the contrast value. Therefore we cannot say that the frequency of the contrast change at the rate of heart beat is induced by only one of them.

The amplitude of the contrast oscillation from 0 to 40 seconds is 0.02 and the modulation depth is 14.3%. However after the deflation of the cuff, the amplitude of the contrast oscillation is only 0.004. Although the contrast value decreased to an average of 0.104, the modulation depth is only 3.8%. This is due to the change of the blood pressure and the circulation. When the blood flow is restricted, less blood flows since the superficial veins are blocked, which also results in higher blood pressure. In addition, the contrast change is partly due to the moving blood cells. When the flow is occluded, the venous blood mean velocity is reduced and the signal is more influenced by the deeper arterial blood. The blood pulsation continues to result mainly from the arteries and the relative oscillation of the contrast is higher.

In this paper, we presented an endoscopic system which can indicate changes of blood volume and flow speed, the heartbeat, respiration and the oxygenation state using LASCA based on the speckle contrast images using lasers at 660nm and 830nm.

REFERENCES

- [1] A. G. Sorensen, W. A. Copen, L. Ostergaard *et al.*, "Hyperacute stroke: Simultaneous measurement of relative cerebral blood volume, relative cerebral blood flow, and mean tissue transit time," *Radiology*, vol. 210, no. 2, pp. 519-527, 1999.
- [2] D. M. Brizel, S. P. Scully, J. M. Harrelson *et al.*, "Tumor oxygenation predicts for the likelihood of distant metastases in human soft tissue sarcoma," *Cancer research*, vol. 56, no. 5, pp. 941-943, 1996.
- [3] J. Wyatt, D. Delpy, M. Cope *et al.*, "Quantification of cerebral oxygenation and haemodynamics in sick newborn infants by near infrared spectrophotometry," *The Lancet*, vol. 328, no. 8515, pp. 1063-1066, 1986.
- [4] A. B. Parthasarathy, S. M. S. Kazmi, and A. K. Dunn, "Quantitative imaging of ischemic stroke through thinned skull in mice with MultiExposure Speckle Imaging," *Biomed. Opt. Express*, vol. 1, no. 1, pp. 246-259.
- [5] S. K. Nadkarni, A. Bilenca, B. E. Bouma *et al.*, "Measurement of fibrous cap thickness in atherosclerotic plaques by spatiotemporal analysis of laser speckle images," *Journal of Biomedical Optics*, vol. 11, no. 2, 2006.
- [6] R. C. Bray, K. R. Forrester, J. Reed *et al.*, "Endoscopic laser speckle imaging of tissue blood flow: Applications in the human knee," *Journal of Orthopaedic Research*, vol. 24, no. 8, pp. 1650-1659, 2006.
- [7] A. A. Kamshilin, S. Miridonov, V. Teplov *et al.*, "Photoplethysmographic imaging of high spatial resolution," *Biomedical optics express*, vol. 2, no. 4, pp. 996-1006.
- [8] R. Bonner, and R. Nossal, "MODEL FOR LASER DOPPLER MEASUREMENTS OF BLOOD-FLOW IN TISSUE," *Applied Optics*, vol. 20, no. 12, pp. 2097-2107, 1981.
- [9] J. D. Briers, "Laser Doppler, speckle and related techniques for blood perfusion mapping and imaging," *Physiological Measurement*, vol. 22, pp. R35, 2001.
- [10] Z. Luo, Z. Yuan, M. Tully *et al.*, "Quantification of cocaine-induced cortical blood flow changes using laser speckle contrast imaging and Doppler optical coherence tomography," *Appl Opt*, vol. 48, no. 10, pp. D247-55, 2009.
- [11] P. Miao, M. H. Li, H. Fontenelle *et al.*, "Imaging the Cerebral Blood Flow With Enhanced Laser Speckle Contrast Analysis (eLASCA) by Monotonic Point Transformation," *Ieee Transactions on Biomedical Engineering*, vol. 56, no. 4, pp. 1127-1133, 2009.
- [12] A. K. Dunn, A. Devor, H. Bolay *et al.*, "Simultaneous imaging of total cerebral hemoglobin concentration, oxygenation, and blood flow during functional activation," *Optics Letters*, vol. 28, no. 1, pp. 28-30, 2003.

- [13] L. Song, and D. Elson, "Endoscopic laser speckle contrast imaging system using a fibre image guide." p. 79070F.
- [14] J. G. Webster, "Medical Instrumentation - Application and Design (4th Edition)," 2010.
- [15] G. Natalini, A. Rosano, M. E. Franceschetti *et al.*, "Variations in arterial blood pressure and photoplethysmography during mechanical ventilation," *Anesthesia & Analgesia*, vol. 103, no. 5, pp. 1182, 2006.
- [16] K. H. Shelley, "Photoplethysmography: beyond the calculation of arterial oxygen saturation and heart rate," *Anesthesia & Analgesia*, vol. 105, no. 6S Suppl, pp. S31, 2007.
- [17] "Tabulated Molar Extinction Coefficient for Hemoglobin in Water, <http://omlc.ogi.edu/spectra/hemoglobin/summary.html>."
- [18] Z. C. Luo, Z. J. Yuan, Y. T. Pan *et al.*, "Simultaneous imaging of cortical hemodynamics and blood oxygenation change during cerebral ischemia using dual-wavelength laser speckle contrast imaging," *Optics Letters*, vol. 34, no. 9, pp. 1480-1482, 2009.
- [19] M. Kohl, U. Lindauer, G. Royl *et al.*, "Physical model for the spectroscopic analysis of cortical intrinsic optical signals," *Physics in Medicine and Biology*, vol. 45, pp. 3749, 2000.
- [20] H. F. Zhang, K. Maslov, M. Sivaramakrishnan *et al.*, "Imaging of hemoglobin oxygen saturation variations in single vessels in vivo using photoacoustic microscopy," *Applied physics letters*, vol. 90, pp. 053901, 2007.